High Metallicity of the X-Ray Gas up to the Virial Radius of a Binary Cluster of Galaxies: Evidence of Galactic Superwinds at High-Redshift

Yutaka Fujita[1], Noriaki Tawa[1], Kiyoshi Hayashida[1], Motokazu Takizawa[2], Hironori Matsumoto[3], Nobuhiro Okabe[4], and Thomas. H. Reiprich[5]

[1]*Department of Earth and Space Science, Graduate School of Science, Osaka University, Toyonaka, Osaka 560-0043*

fujita@vega.ess.sci.osaka-u.ac.jp

[2]*Department of Physics, Yamagata University, Yamagata 990-8560*

[3]*Department of Physics, Kyoto University, Kitashirakawa, Sakyo-ku, Kyoto 606-8502*

[4]*Astronomical Institute, Graduate School of Science, Tohoku University, Sendai 980-8578*

[5]*Argelander Institute for Astronomy (AIfA), Bonn University, Auf dem Hügel 71, 53121 Bonn, Germany*

(Received 2007 March 25; accepted 2007 May 12)

Abstract

We present an analysis of a Suzaku observation of the link region between the galaxy clusters A 399 and A 401. We obtained the metallicity of the intracluster medium (ICM) up to the cluster virial radii for the first time. We determine the metallicity where the virial radii of the two clusters cross each other (~ 2 Mpc away from their centers) and found that it is comparable to that in their inner regions ($\sim 0.2\,Z_\odot$). It is unlikely that the uniformity of metallicity up to the virial radii is due to mixing caused by a cluster collision. Since the ram-pressure is too small to strip the interstellar medium of galaxies around the virial radius of a cluster, the fairly high metallicity that we found there indicates that the metals in the ICM are not transported from member galaxies by ram-pressure stripping. Instead, the uniformity suggests that the proto-cluster region was extensively polluted with metals by extremely powerful outflows (superwinds) from galaxies before the clusters formed. We also searched for the oxygen emission from the warm–hot intergalactic medium in that region and obtained a strict upper limit of the hydrogen density ($n_{\rm H} < 4.1 \times 10^{-5}\,{\rm cm}^{-3}$).

Key words: galaxies: clusters: general—galaxies: evolution— galaxies: intergalactic medium— X-rays: galaxies: clusters— galaxies: clusters: individual (A 399, A 401)

1. Introduction

Clusters of galaxies are filled with hot X-ray gas ($\sim$ 2–10 keV), which is often called the intracluster medium (ICM) (Sarazin 1986). In the inner region of clusters ($r \lesssim 0.4\,r_{\rm vir}$, where $r_{\rm vir}$ is the virial radius), the average metallicity of the ICM is $\sim 0.3\,Z_{\odot}$ (Arnaud et al. 1992; Fukazawa et al. 2000). The metals in the ICM were originally produced by stars in galaxies. However, it is still unclear how and when they were transported into the hot gas from the galaxies. Possible mechanisms that transfer metals from the cluster galaxies into the surrounding gas can be classified broadly into two types, ram-pressure stripping and energetic outflows from the galaxies. In the former, a galaxy is moving in the ICM and the metal-enriched gas in the galaxy (interstellar medium) is stripped by ram-pressure from the ICM (Gunn, Gott 1972; Fujita, Nagashima 1999; Quilis et al. 2000). The larger is the density of the ambient ICM and/or the relative velocity between the galaxy and the ICM, the larger is the ram-pressure affecting the galaxy. Thus, ram-pressure stripping is most effective at the cluster center. In the latter, supernova explosions following active star formation in a galaxy drive outflows, and the metals are carried by them (De Young 1978). Since the static pressure from the ICM suppresses the development of the outflows, the latter mechanism is rather effective in the peripheral region of a cluster, or the intergalactic space before the cluster forms (a proto-cluster region) (Kapferer et al. 2006). Therefore, it is critical to determine the metallicity of the ICM in the outermost region ($r \sim r_{\rm vir}$) of clusters in order to know which mechanism is dominant. Unfortunately, previous observations of metallicity have been limited to the inner region of clusters ($r \lesssim 0.4\,r_{\rm vir}$) (De Grandi et al. 2004; Pratt et al. 2007).

In order to study the nature of the ICM far away from cluster centers, we observed the link region between two clusters, A 399 and A 401. Their redshifts are $z = 0.0718$ (A 399) and 0.0737 (A 401) (Oegerle, Hill 2001). In this paper, we assume cosmological parameters of $\Omega_0 = 0.3$, $\lambda = 0.7$, and $H_0 = 70\,{\rm km\,s^{-1}\,Mpc^{-1}}$. For those parameters, the projected distance between the two clusters is 3 Mpc. Previous X-ray observations showed that these clusters are massive, and the temperatures are 7.23 keV (A 399) and 8.47 keV (A 401) (Sakelliou, Ponman 2004). They indicated that the clusters are at an initial stage of a cluster merger, and that the hot gas in the link region is slightly compressed (Sakelliou, Ponman 2004; Fujita et al. 1996). Since Suzaku has a large collecting area and low background (Mitsuda et al. 2007), it is the best instrument for observations of dim and diffuse X-ray emission, such as that from the ICM in the periphery of a cluster.

It is believed that there is a warm–hot intergalactic medium (WHIM) around clusters, which is theoretically predicted, and is known as a candidate for the "missing baryon" in the Universe (Cen, Ostriker 1999). While there have been several reports claiming detection (Finoguenov et al. 2003; Kaastra et al. 2003; Fujimoto et al. 2004; Nicastro et al. 2005; Takei et al. 2007b), there have been arguments against them (Bregman, Lloyd-Davies 2006; Kaastra et

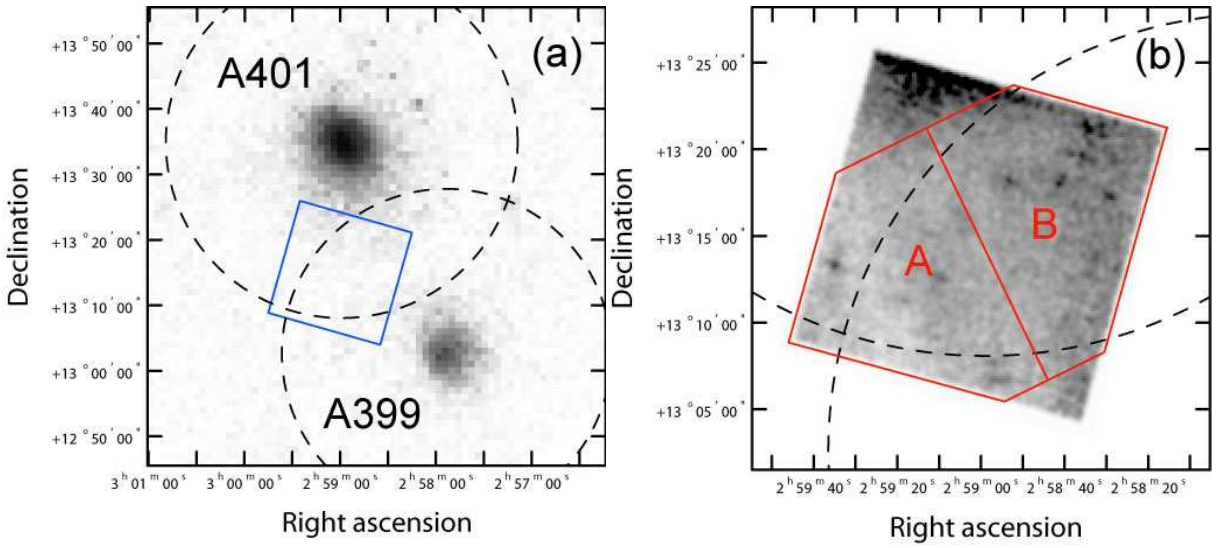

Fig. 1. (a) ROSAT PSPC image of A 399/A 401. The virial radii of the clusters are shown by dashed-line circles. The Suzaku field shown in figure 1b is indicated by a solid-line square. (b) Suzaku image of the link region. The background and vignetting are corrected. The virial radii of the clusters are shown by dashed-line circles. Regions used for spectral analysis are labeled "A" and "B".

al. 2006; Takei et al. 2007a). One difficulty in detecting the emission or absorption of the WHIM is discrimination from the emission or absorption of the Galactic warm gas. Since Suzaku has a good energy resolution of $\Delta z \sim 0.01$ even in the energy band of < 1 keV, it can in principal discriminate extragalactic WHIM at $z \sim 0.07$ from the Galactic warm gas at $z = 0$ in redshift space.

This paper is organized as follows. The observations are presented in section 2. In section 3, the metallicity of the ICM in the outermost region of the clusters and the line emission from the WHIM are considered. Section 4 is devoted to discussion. Conclusions are summarized in section 5.

2. Observations

We observed the link region with Suzaku on 2006 August 19–22 for an exposure time of 150 ks. The field of view of Suzaku XIS CCDs is shown in a ROSAT PSPC image (figure 1a). The region that we observed is the outermost region of the two clusters, where their virial radii cross each other. The virial radii are approximated by those inside which the mean mass density is 200-times the critical density of the Universe. They are $r_{\rm vir} = 2.16$ Mpc for A 399 and 2.34 Mpc for A 401 (Sakelliou, Ponman 2004). Because of the projection and the interaction of the two clusters, the region is brighter than the other sides of the clusters for a given a distance from the cluster centers (Fujita et al. 1996; Sakelliou, Ponman 2004). The gas that was in the cosmological filament that connected the two clusters might have been compressed.

Suzaku has four XIS CCDs (Koyama et al. 2007). Three of them are front-illuminated

(FI) and one is back-illuminated (BI). The former have a higher sensitivity at the high -nergy band ($\gtrsim 2$ keV) than the latter, and the latter has a higher sensitivity at the low energy band ($\lesssim 2$ keV). Therefore, we used the three FIs to study the hot ICM (subsection 3.1) and the BI to study the WHIM (subsection 3.2).

The XIS was operated in the normal full-frame clocking mode. The edit mode was 3×3 and 5×5, and we combined the data of both modes for our analysis. We employed revision 1.2 of the cleaned event data. Events with ASCA grades of 0, 2, 3, 4, and 6 were retained. We excluded the data obtained at the South Atlantic Anomaly, during Earth occultation, and at the low elevation angles from Earth rims of $< 5^\circ$ (night Earth) and $< 20^\circ$ (day Earth). Figure 1b is the summed image of the three FIs (0.4–5 keV). Although the north (the region closer to A 401) is brighter than the south-east corner, noticeable structures, such as a group of galaxies, are not seen.

3. Spectral Analysis

3.1. The ICM in the Link Region

We extracted spectra for regions A and B (see figure 1b) in the 0.4–10 keV band. Since the X-rays from the link region is diffuse and extended, we calculated the effective area for each XIS chip using XISSIMARFGEN (version 2006-11-26), which provides the ancillary response file (ARF) through Monte Carlo simulations. Based on the beta model parameters and temperatures (Sakelliou, Ponman 2004), we also calculated the contamination of photons from the bright centers of the clusters by simulating the number of photons from outside of the Suzaku field. Although we found that it is only 4% of the total photons in the Suzaku field, we included the effect of the contaminating photons in the ARF.

Non-X-ray instrumental background (NXB) was subtracted from the spectrum of the link region using night Earth data. However, the NXB data provided by the Suzaku team were based on the night Earth data taken from September 2005 to May 2006, and we found that some corrections were required to apply them to our observations made in August 2006 (Tawa et al. 2008). The problem is caused by the attenuation of metal lines scattered from the calibration source and the degradation of spectral resolution of XIS.

First, we fit the lines in the NXB spectrum with Gaussian profiles using the redistribution matrix file (RMF) of 2005 August, which was suitable for the spectral analysis of data taken in the period when the night Earth data were taken. The normalization and width of the lines were not fixed in the fit. Next, we subtracted the lines from the NXB spectrum and obtained the continuum spectrum of the NXB. For the Mn lines from the calibration source, we considered the radioactive decay of Mn (the half period is 2.73 yr). For prominent lines, we consider the degradation of the spectral resolution of XIS. Then, we simulated the line profiles in 2006 August. Finally, adding the simulated lines to the continuous spectrum of the NXB,

we obtain the corrected NXB background; we used it for the following spectral analysis.

In the spectral analysis, X-ray point sources in the field were removed. For each region (A and B), the spectra of the three FIs were summed. Using XSPEC (version 12), the summed spectra were fitted with a single thermal model (APEC) representing the ICM and with Galactic absorption (WABS). While the redshift of the ICM ($z = 0.073$) and the Galactic absorption ($N_{\rm H} = 1 \times 10^{21}\,{\rm cm}^{-2}$; Dickey, Lockman 1990) were fixed in the fits, the temperature and metallicity of the ICM were free. In the fits, we also considered the contributions of the cosmic X-ray background (CXB) obtained by ASCA (Kushino et al. 2002) and the Galactic soft X-ray emission[1]. The CXB spectrum is given by a power-law with an index of 1.412, and the flux in the 2–10 keV band is $F_{\rm CXB} = 6.38 \times 10^{-8}\,{\rm erg\,cm^{-2}\,s^{-1}\,sr^{-1}}$. We call this CXB spectrum 'the fiducial CXB spectrum'. The Galactic soft X-ray emission consists of two thermal components of $T = 0.0827$ (the local hot bubble) and 0.184 keV (the Milky Way halo) (Snowden et al. 1998). The metallicity and the redshift of the both components are one solar abundance and zero, respectively. The parameters for the Galactic soft X-ray emission were fixed in the fits, except for the overall normalization; the relative normalization between the two components was fixed at 1.04, which is provided by the Galactic soft X-ray emission model [1]. The following results about the hot ICM are not sensitive to the Galactic soft X-ray emission. Figure 2 shows the summed spectrum of the three FIs for region A and the result of the fit; an Fe K line is clearly seen. We fixed the CXB spectrum at the fiducial one. For this fit, $\chi^2/{\rm dof} = 1844.60/1731$.

In figure 3, we present the temperatures and metallicities of regions A and B. When we derived the error bars, we varied the normalization of the CXB in order to involve any possible field-to-field variance. Kushino et al. (2002) estimated that the intensity changed $6.49^{+0.56}_{-0.61}\%$ for the ASCA field ($\sim 0.5\,{\rm deg}^2$). The area of regions A and B is $\sim 0.04\,{\rm deg}^2$. Assuming that the CXB intensity follows the Poisson model, the CXB uncertainty for regions A and B is $\sim 6.5\sqrt{0.5/0.04} \approx 23\%$. Conservatively, we take an uncertainty of 30%. We fit the XIS spectra of regions A and B for 30% higher or lower CXB normalizations than that of the fiducial CXB spectrum and derive temperatures and metallicities. Adding the statistical errors of the fits to this CXB uncertainty, we obtained the error bars in figure 3.

In that figure, we compare the temperatures and metallicities in the link region with the average ones of the inner regions of A 399 and A 401 ($r \lesssim 0.4\,r_{\rm vir}$) (Sakelliou, Ponman 2004). The temperatures of regions A and B would have been raised slightly from their original values because of gas compression associated with the interaction between the two clusters. The metallicities of regions A and B ($\sim 0.2\,Z_\odot$) are not different from those in their inner regions.

[1] http://heasarc.gsfc.nasa.gov/cgi-bin/Tools/xraybg/xraybg.pl.

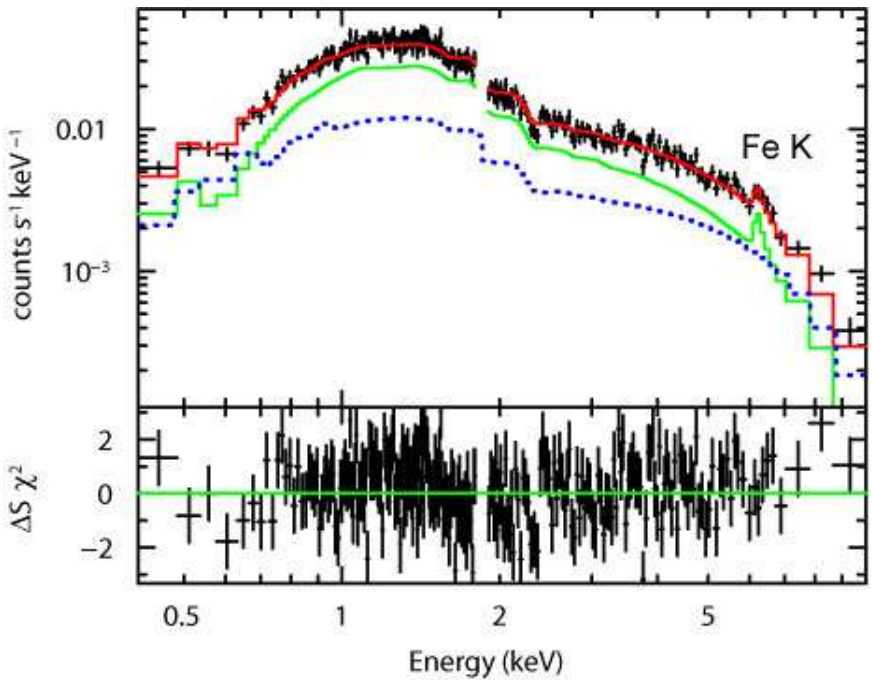

Fig. 2. X-ray spectrum of region A shown in figure 1b (crosses). Three FI XIS spectra were summed. The result of the fit is shown by the red line, while the lower panel plots the residuals divided by the 1σ errors. The green solid line shows the contribution of the ICM, and the blue dotted line shows the contribution of CXB and Galactic emission. The excess seen at $\gtrsim 6$ keV, which is also seen in figure 4, may be due to the field-to-field variation of the CXB strength (see text).

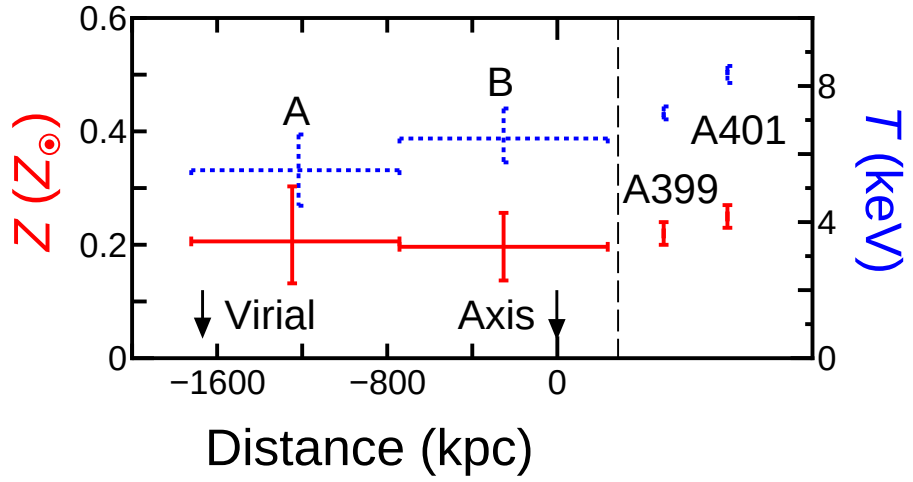

Fig. 3. Temperatures (blue, dotted) and metallicities (red, solid) of regions A and B. Those of the inner regions of A 399 and A 401 are also shown for comparison (Sakelliou, Ponman 2004). The abscissa axis is the distance from the line connecting the two cluster centers ("Axis"). The position where the virial radii of the two clusters cross each other is referred as "Virial". The error bars are 90% confidence intervals.

3.2. Warm-Hot Intergalactic Medium

The high ICM metallicity observed in the link region ($\sim 0.2\,Z_\odot$) may indicate that the WHIM around clusters would also be highly polluted with metals (Cen, Ostriker 2006). Thus, the metal line emission from the WHIM could be detected (Yoshikawa et al. 2003). We searched for O VII line emission from the WHIM around the binary cluster superposed on the Suzaku field.

At the redshift of the link region ($z \sim 0.073$), the O VII line (intrinsically 0.57 keV) would be observed at 0.53 keV. Unfortunately, X-ray spectra in the energy band of $\lesssim 1$ keV are often affected by the solar wind (Fujimoto et al. 2007). The level 2 ACE SWEPAM data[2] show that in the first half of our observation time, the proton flux is $\sim 5 \times 10^8\,\mathrm{cm^{-2}\,s^{-1}}$, which is comparable to the level when solar-wind charge-exchange X-ray emission from the Earth's magnetosheath was observed (Fujimoto et al. 2007). In fact, we found that the XIS photon counts in the 0.3–1 keV band are $\sim 20\%$ larger in the first half of our observation time than those in the second half. Thus, we used only the data of the second half of our observation time (75 ks), because they are less affected by the solar wind. We apply the analysis in subsection 3.1 to the BI.

The BI spectrum of the entire Suzaku field (figure 1) was fitted in the 0.25–8 keV band with a single thermal model (APEC), a Gaussian corresponding to the expected O VII line around 0.53 keV, and other components not relating to the binary cluster (the CXB, the Galactic soft X-ray emission, and the Galactic absorption). The thermal component is required to precisely estimate the contribution of the hot ICM. We assumed that the metallicity and redshift of the thermal component are $Z = 0.2\,Z_\odot$ and $z = 0.073$, respectively. The former is the ICM metallicity derived with FI (subsection 3.1). The temperature and normalization of the thermal component were free in the fit. While the unknown intrinsic width of the Gaussian component was fixed at zero, the line center and normalization of the component were not fixed. The parameters for the CXB, the Galactic soft X-ray emission, and the Galactic absorption were the same as those in the previous analysis for the FIs. The overall normalization of the Galactic soft X-ray emission was varied. When we derived error bars for the temperature of the thermal component and the strength of the O VII line emission from the WHIM, the 30% uncertainty of the CXB was considered.

The result of the fit is shown in figure 4. For this fit, $\chi^2/\mathrm{dof} = 524.98/477$. The temperature of the thermal component is $T = 5.8^{+0.9}_{-0.9}$ keV. No line is seen at 0.53 keV. Another thermal component that may represent the WHIM is not required. Although we have tried to fit the FI and BI spectra simultaneously, the results were not improved.

[2] http://swepam.lanl.gov/data/raw/index.cgi/swepam_dswi_level2.

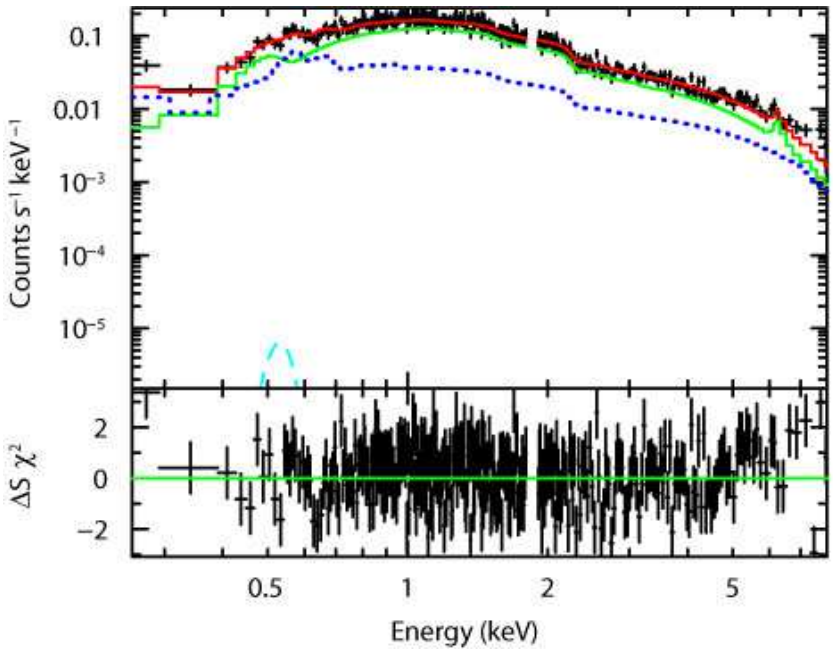

Fig. 4. Same as figure 2 but for the BI spectrum of the entire Suzaku field. The contribution of the Gaussian component shown at 0.53 keV is that when the line center energy was fixed at 0.53 keV.

4. Discussion

4.1. The High Metallicity of the ICM

Figure 3 suggests that the metallicity of the ICM is uniform up to the virial radii of the two clusters. Since the surface brightness of a cluster is a decreasing function of the radius, the fraction of photons coming from the virial radii may not be large in the Suzaku field. However, they come from at least $r \geq 0.5\, r_{\rm vir}$ (see Fig. 1), where the metallicity has not been obtained before. The uniformity could be due to a head-on collision of the two clusters; if the two clusters had already passed through each other, metal-rich gas would have been pulled out of their central regions. However, numerical simulations showed that while collisionless dark matter and galaxies can pass through the other cluster at a cluster collision, collisional ICM cannot. Thus, the ICM is detached from the dark matter and galaxies (Takizawa 1999; Ricker, Sarazin 2001; Poole et al. 2006). However, X-ray observations have shown that the overall X-ray morphology of the two clusters is regular (figure 1a), which indicates that the ICM is almost in pressure equilibrium in the gravitational potentials formed by the dark matter (Sakelliou, Ponman 2004). Moreover, their X-ray centers are coincident with their central galaxies as is the case of non-merging clusters (Fujita et al. 1996). These indicate that the clusters have not passed through each other. Although both A 399 and A 401 do not have a prominent cool core, Sakelliou and Ponman (2004) concluded that this is because each cluster has undergone minor mergers, which did not significantly affect the overall structures. Still, we cannot rule

out that the minor mergers might have resulted in some mixing of metals. It is, therefore, important that the findings here also be confirmed with classical relaxed clusters. Moreover, we determined only the metallicity of the link region. Those on the other sides of both clusters should be determined in the future.

It is also unlikely that the high metallicity observed with Suzaku is due to a small-scale structure with high metallicity. Figure 1 shows that there is no noticeable X-ray structure in the Suzaku field. Moreover, there is no enhancement of the number density of galaxies in that region (Sakelliou, Ponman 2004). These results mean that there is no group of galaxies that possibly ejects more metals than the surrounding region. Furthermore, there is no difference of metallicity between regions A and B (figure 3). This shows that the metallicity is uniform at least on a scale of ~ 1 Mpc.

If the metallicity is actually high in the outermost region other than the link region, and if the high metallicity is not due to cluster mergers, it constrains models of metal transportation from galaxies. First, ram-pressure stripping is rejected as the main mechanism, because the ram-pressure is very small and the stripping is ineffective at $r \sim r_{\rm vir}$ (Fujita, Nagashima 1999; Domainko et al. 2006). Note that although the two clusters are interacting, they are just at an initial stage of a collision. Using the beta model parameters for both clusters obtained by Sakelliou and Ponman (2004), the summed ICM density in the Suzaku field is $\sim 2.4 \times 10^{-4}\,{\rm cm}^{-3}$. Since the surface brightness in the field is a factor of two larger than the simple superposition of the two clusters (figure 10 in Sakelliou, Ponman 2004), the actual density would be $\sqrt{2}$ times larger, and be $\sim 3.4 \times 10^{-4}\,{\rm cm}^{-3}$. For a typical galaxy, ram-pressure stripping happens when the ram-pressure exceeds $\sim 2 \times 10^{-11}\,{\rm dyne\,cm}^{-2}$ (Fujita, Nagashima 1999). Thus, the relative velocity between a galaxy and the ICM must be larger than $\sim 2000\,{\rm km\,s}^{-1}$ for effective ram-pressure stripping. It is unlikely that this happens at this stage of a cluster collision (Fujita et al. 1999).

Therefore, outflows from galaxies are the most promising candidates of the metal transportation mechanism. However, theoretical studies have shown that simple galactic-outflow models using standard parameters for star formation do not reproduce the level of uniformity that we observed. They predict that metallicity in the outermost region of a cluster should be at least a factor of a few smaller than the average metallicity in the inner region ($r \lesssim 0.4\,r_{\rm vir}$) (Tornatore et al. 2004; Kapferer et al. 2006). In particular, metal maps obtained by the latest numerical simulations [e.g. figures 5 and 6 of Kapferer et al. (2007)] showed that metals are concentrated in the central regions ($\lesssim 1$ Mpc) of clusters with temperatures of $T \sim 8$ keV, except for small substructures with a size of ~ 0.5 Mpc. The reason is that in these models most metals are produced by galaxies within an already formed cluster potential well and the ICM at $z < 1$–2. Thus, it is difficult for ordinary outflows to transfer metals away from galaxies. In particular, elliptical galaxies, which are often thought to be the main metal sources of the ICM (Arnaud et al. 1992), are concentrated in the central regions of clusters at $z \sim 0$ (e.g. Goto

et al. 2003). It is not feasible for the elliptical galaxies in the grown-up clusters to pollute the ICM at $r \sim r_{\rm vir}$ with metals. For example, an elliptical galaxy with a luminosity of $L_{\rm B} = 10^{10}\,L_{\odot}$ releases an energy of $E_{\rm w} \sim 10^{60}$ erg through galactic outflow (David et al. 1991). The distance from the galaxy to which the outflow can reach, $d_{\rm w}$, has the relation

$$E_{\rm w} \sim (4\pi/3) P d_{\rm w}^3\,, \tag{1}$$

where P is the pressure of the ICM surrounding the galaxy. Thus,

$$d_{\rm w} \sim 86 \left(\frac{n}{10^{-3}\,{\rm cm}^{-3}}\right)^{-1/3} \left(\frac{T}{8\,{\rm keV}}\right)^{-1/3} \left(\frac{E_{\rm w}}{10^{60}\,{\rm erg}}\right)^{1/3} {\rm kpc}\,, \tag{2}$$

where n is the density of the ICM surrounding the galaxy. The distance $d_{\rm w}$ is much smaller than the virial radius of a cluster (~ 2 Mpc), which shows that the galactic outflows from elliptical galaxies at $z \sim 0$ alone cannot explain the high metallicity observed at $r \sim r_{\rm vir}$.

The solution may be extremely powerful outflows from galaxies at high-redshifts ($z \sim 2$). At that time, clusters had not much grown, and most galaxies observed in clusters at $z \sim 0$ had not fallen into the clusters. Such outflows (superwinds) could be produced by active galactic nuclei (AGNs) or intensive starburst activities (Benson et al. 2003; Cen, Ostriker 2006), and they could pollute gas with metals throughout the proto-cluster region (Romeo et al. 2006; Moll et al. 2007). That metal-enriched gas would be captured by A 399 and A 401 recently, and would be observed as the ICM at present. In fact, the space density of luminous AGNs and that of starburst galaxies increase from $z = 0$ to $z \sim 2$ (Ueda et al. 2003; Franceschini et al. 2001). Using semi-analytical galaxy formation models, Nagashima et al. (2005) indicated that the metals were ejected into space outside the cluster ancestors by superwinds before the circular velocity of the individual ancestors increased to $\sim 600\,{\rm km\,s^{-1}}$.

4.2. Warm-Hot Intergalactic Medium

We estimated the upper limit of the O VII line emission from the WHIM. Figure 5 shows the confidence contours for the line center energy and the normalization. While there is no structure around 0.53 keV, there is a noticeable structure at ~ 0.57 keV. Thus, the possible line in the spectrum could be associated with an insufficient correction of the Galactic soft X-ray emission. If we assume that the center of the line is at 0.53 keV, the line strength is $I < 8.0 \times 10^{-8}\,{\rm photons\,cm^{-2}\,s^{-1}\,arcmin^{-2}}$ (90% confidence level). Assuming that the temperature of the gas associated with the O VII line is $T = 2 \times 10^6$ K, the hydrogen density at $z = 0.073$ can be represented by

$$n_{\rm H} = 9.2 \times 10^{-5} {\rm cm}^{-3} \left(\frac{I}{1 \times 10^{-7} {\rm ph\,cm^{-2}\,s^{-1}}}\right)^{1/2} \left(\frac{Z}{0.1\,Z_{\odot}}\right)^{-1/2} \left(\frac{L}{1\,{\rm Mpc}}\right)^{-1/2}, \tag{3}$$

where L is the path length (Takei et al. 2007a). From equation (3), the density of the WHIM is $n_{\rm H} < 4.1 \times 10^{-5}\,{\rm cm^{-3}}$ for $Z = 0.2\,Z_{\odot}$ and $L = 2$ Mpc. The value of Z is the ICM metallicity obtained with FIs and that of L is the typical depth of warm gas in a cosmic filament (Colberg

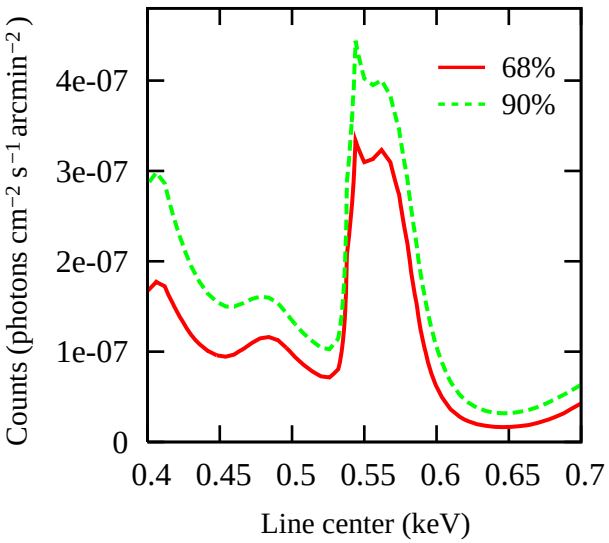

Fig. 5. Confidence contours for the line center and photon counts of the Gaussian component. The lines show 68% and 90% confidence regions for two interesting parameters. For this figure, the 30% uncertainty of the CXB is not considered, because we found that the effect is negligible.

et al. 2005).

The allowed density is smaller than that of the hot ICM in the link region ($n_{\rm H} \sim 3.4 \times 10^{-4}\,{\rm cm}^{-3}$; see section 4). The upper limit is also smaller than that obtained for A2218 ($n_{\rm H} < 5.5 \times 10^{-5}\,{\rm cm}^{-3}$ for $Z = 0.2\,Z_{\odot}$, and $L = 2$ Mpc; Takei et al. 2007a). It is to be noted that since the emissivity of the O VII line is peaked at $T \approx 2 \times 10^6$ K, the hydrogen density could be larger if the temperature of the WHIM is much different from $T = 2 \times 10^6$ K.

5. Conclusions

We observed the link region between massive clusters A 399 and A 401 with the XIS instrument aboard Suzaku. We measured the metallicity of the hot ICM where the virial radii of the two clusters cross each other, and found that it is $\sim 0.2\,Z_{\odot}$, which is comparable to those in the inner regions of the clusters. This suggests that the metallicity is uniform within the virial radii. The X-ray morphology of the two clusters indicates that the uniformity of the metallicity is not due to a major cluster merger. The fairly high metallicity in the outermost region of the clusters shows that ram-pressure stripping is not the main mechanism that transports metals from galaxies to the hot ICM. Moreover, the uniformity suggests that the metals were not ejected through ordinary galactic outflows after the clusters formed. It is more likely that the metals were carried by galactic superwinds before the clusters formed, and that the proto-cluster region was heavily polluted with the metals.

We also searched for the oxygen emission from the WHIM around the clusters. We could obtain a strict constraint of the density of the WHIM, which is $n_{\rm H} < 4.1 \times 10^{-5}\,{\rm cm}^{-3}$.

The authors wish to thank the referee for useful comments. We also thank the Suzaku operations team for their support in planning and executing these observations. Y. F., K. H., and M. T. were supported in part by a Grant-in-Aid from the Ministry of Education, Culture, Sports, Science and Technology of Japan (Y. F.: 17740162; K. H.:16002004; M. T.: 16740105, 19740096). T. H. R. acknowledges support by the Deutsche Forschungsgemeinschaft through Emmy Noether Research Grant RE 1462.

References

Arnaud, M., Rothenflug, R., Boulade, O., Vigroux, L., & Vangioni-Flam, E. 1992, A&A, 254, 49
Benson, A. J., Bower, R. G., Frenk, C. S., Lacey, C. G., Baugh, C. M., & Cole, S. 2003, ApJ, 599, 38
Bregman, J. N., & Lloyd-Davies, E. J. 2006, ApJ, 644, 167
Cen, R., & Ostriker, J. P. 1999, ApJ, 514, 1
Cen, R., & Ostriker, J. P. 2006, ApJ, 650, 560
Colberg, J. M., Krughoff, K. S., & Connolly, A. J. 2005, MNRAS, 359, 272
David, L. P., Forman, W., & Jones, C. 1991, ApJ, 380, 39
De Grandi, S., Ettori, S., Longhetti, M., & Molendi, S. 2004, A&A, 419, 7
De Young, D. S. 1978, ApJ, 223, 47
Dickey, J. M., & Lockman, F. J. 1990, ARA&A, 28, 215
Domainko, W., et al. 2006, A&A, 452, 795
Finoguenov, A., Briel, U. G., & Henry, J. P. 2003, A&A, 410, 777
Franceschini, A., Aussel, H., Cesarsky, C. J., Elbaz, D., & Fadda, D. 2001, A&A, 378, 1
Fujimoto, R., et al. 2004, PASJ, 56, L29
Fujimoto, R., et al. 2007, PASJ, 59, S133
Fujita, Y., Koyama, K., Tsuru, T., & Matsumoto, H. 1996, PASJ, 48, 191
Fujita, Y., & Nagashima, M. 1999, ApJ, 516, 619
Fujita, Y., Takizawa, M., Nagashima, M., & Enoki, M. 1999, PASJ, 51, L1
Fukazawa, Y., Makishima, K., Tamura, T., Nakazawa, K., Ezawa, H., Ikebe, Y., Kikuchi, K., & Ohashi, T. 2000, MNRAS, 313, 21
Goto, T., Yamauchi, C., Fujita, Y., Okamura, S., Sekiguchi, M., Smail, I., Bernardi, M., & Gomez, P. L. 2003, MNRAS, 346, 601
Gunn, J. E., & Gott, J. R., III 1972, ApJ, 176, 1
Kaastra, J. S., Lieu, R., Tamura, T., Paerels, F. B. S., & den Herder, J. W. 2003, A&A, 397, 445
Kaastra, J. S., Werner, N., den Herder, J. W. A., Paerels, F. B. S., de Plaa, J., Rasmussen, A. P., & de Vries, C. P. 2006, ApJ, 652, 189
Kapferer, W., et al. 2006, A&A, 447, 827
Kapferer, W., et al. 2007, A&A, 466, 813
Koyama, K., et al. 2007, PASJ, 59, S23
Kushino, A., Ishisaki, Y., Morita, U., Yamasaki, N. Y., Ishida, M., Ohashi, T., & Ueda, Y. 2002, PASJ, 54, 327
Mitsuda, K., et al. 2007, PASJ, 59, S1

Moll, R., et al. 2007, A&A, 463, 513
Nagashima, M., Lacey, C. G., Baugh, C. M., Frenk, C. S., & Cole, S. 2005, MNRAS, 358, 1247
Nicastro, F., et al. 2005, Nature, 433, 495
Oegerle, W. R., & Hill, J. M. 2001, AJ, 122, 2858
Poole, G. B., Fardal, M. A., Babul, A., McCarthy, I. G., Quinn, T., & Wadsley, J. 2006, MNRAS, 373, 881
Pratt, G. W., Böhringer, H., Croston, J. H., Arnaud, M., Borgani, S., Finoguenov, A., & Temple, R. F. 2007, A&A, 461, 71
Quilis, V., Moore, B., & Bower, R. 2000, Science, 288, 1617
Ricker, P. M., & Sarazin, C. L. 2001, ApJ, 561, 621
Romeo, A. D., Sommer-Larsen, J., Portinari, L., & Antonuccio-Delogu, V. 2006, MNRAS, 371, 548
Sakelliou, I., & Ponman, T. J. 2004, MNRAS, 351, 1439
Sarazin, C. L. 1986, Rev. Mod. Phys., 58, 1
Snowden, S. L., Egger, R., Finkbeiner, D. P., Freyberg, M. J., & Plucinsky, P. P. 1998, ApJ, 493, 715
Takei, Y., et al. 2007a, PASJ, 59, S339
Takei, Y., Henry, J. P., Finoguenov, A., Mitsuda, K., Tamura, T., Fujimoto, R., & Briel, U. G. 2007b, ApJ, 655, 831
Takizawa, M. 1999, ApJ, 520, 514
Tawa, N., et al. 2008, PASJ, 60, S11
Tornatore, L., Borgani, S., Matteucci, F., Recchi, S., & Tozzi, P. 2004, MNRAS, 349, L19
Ueda, Y., Akiyama, M., Ohta, K., & Miyaji, T. 2003, ApJ, 598, 886
Yoshikawa, K., Yamasaki, N. Y., Suto, Y., Ohashi, T., Mitsuda, K., Tawara, Y., & Furuzawa, A. 2003, PASJ, 55, 879